Cascade process of two-dimensional turbulence observed in magnetized pure electron plasmas

Yosuke KAWAI[1)], Yasuhito KIWAMOTO[1)], Yukihiro SOGA[1)*]and Jun AOKI[1)*]

[1)]*Graduate School of Human and Environmental Studies, Kyoto University, Yoshida Nihonmatsu-cho, Sakyo-ku, Kyoto 606-8501, Japan*

(15 October 2007)

Elementary dynamics of two-dimensional (2D) turbulence are examined experimentally by extensive analyses of fine-scale structures in the density distribution of a magnetized pure electron plasma. We observe the relaxation process of the electron plasma involving stochastic mergers of vortex patches generated by the instability in terms of a spatial pattern of vorticity, and compare with the theoretical picture of the 2D turbulence described in the wave-number (k) space. In the merging process among vortex patches, the energy spectrum shows a algebraic dependence of $k^{-\alpha}$ above the k_{inj} corresponding to the size of the first generated patches. The energy and enstrophy tranfer rate show the characteristic features of the cascade process predicted by the theory, i.e., in the fine-length scale of $k > k_{inj}$ the enstrophy cascades upward at a constant transfer rate, and in the region $k < k_{inj}$ the energy transfers down to lower k. Through time-averaging the evolution of the spectra, we derive the spectrum in the stationary turbulence sustained by the successive input of vortices due to the instability. The resultant spectrum is qualitatively consistent with the 2D turbulence theory, but also shows the discrepancies that the power index of the energy spectrum is larger than the theoretical prediction of $\alpha = 3$ and that the enstrophy transfer rate is almost zero around $k \approx k_{inj}$ reflecting the effect of coherent vortices.

Keywords: non-neutral plasmas, two-dimensional turbulence, vortex dynamics, spectral analysis, enstrophy cascade

DOI:

Macroscopic dynamics of pure electron plasmas transverse to a strong magnetic field are equivalent to the two-dimensional (2D) Euler fluid within the guiding-center approximation, and the electron density $n(x, y)$ and the potential distribution $\phi(x, y)$ are proportional to the vorticity $\zeta(x, y)$ and the stream function $\psi(x, y)$, respectively [1, 2]. Taking advantage of this equivalence, magnetized pure electron plasmas have been employed extensively for detailed examinations of many aspects of 2D vortical dynamics, that constitute the elementary processes of 2D turbulence, such as the advection, merger, filamentation of vortices [2–4]

Vortex patches are spontaneously generated in the nonlinear stage of the diocotron instability from the ring-shaped electron density with a strong radial shear of the azimuthal flow [1, 5]. Free relaxations of the unstable system include stochastic dynamics of vortex patches. Time-resolved spectral analyses have been carried out along the relaxation of the turbulent states, focusing on the particle transport [6]. In this paper, we extend these examinations further to explore fundamental properties of 2D turbulence of the vorticity distribution in terms of the transport of the energy and enstrophy in the wave-number (k) space.

*Present address: Department of Physics, Graduate School of Science, Osaka University, 1-1 Machikaneyama, Toyonaka, Osaka 560-0043, Japan
author's e-mail: kwaiyosuke@h01a0395.mbox.media.kyoto-u.ac.jp

Theoretical picture of 2D turbulence have been conjectured by Kraichnan [7] and Batchelor [8]. Both of them proposed that in the isotropic and homogeneous 2D turbulence, the enstrophy injected at the length-scale of l_{inj} ($\propto 1/k_{inj}$) cascades at a constant transfer-rate of η down to a scale of dissipation l_d ($\propto 1/k_d$) and dissipates by viscosity. This cascade picture of 2D turbulence leads to an energy spectrum characterized by the power-law $E(k) \propto k^{-3}$ in the inertial range of $k_{inj} \leq k \leq k_d$ in the wave-number space.

The cascade process of the enstrophy has been investigated experimentally by using thin layers of electrolytes [9, 10] and soap films [11], and k^{-3} scaling has been observed. However, in these experiments, it is difficult to resolve the fine vortical structures extending to the dissipative range, and therefore there remains some uncertainties in comparing the vortex dynamics observed in the real space with the theoretical picture of 2D turbulence described in the spectral space.

In the experimental investigation with pure electron plasmas, the vorticity distribution can be observed directly in terms of the electron density distribution $n(x, y)$ down to the dissipative scale at a high signal-to-noise ratio. With this advantage, in this paper, we examine the cascade process of the free-decaying 2D turbulence extensively in wide length scales. Moreover, by considering this phenomena as an elementary process of forced 2D turbulence, we

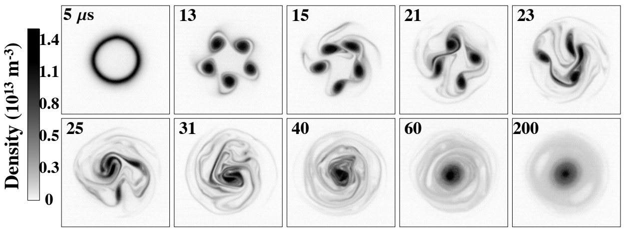

Fig. 1 Images of the time evolution of the density distribution. The darkness is proportional to the density. The time of observation (in μs) is indicated at the upper left corner.

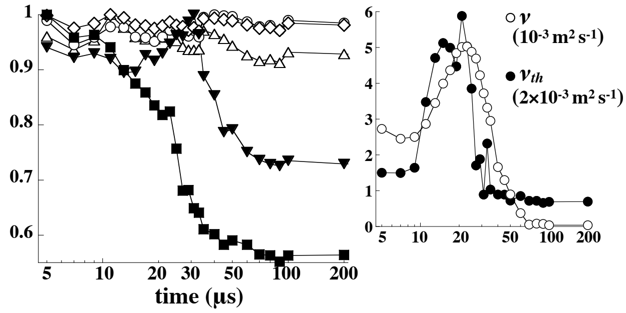

Fig. 2 The time evolution of energy E (○), total electron number N (◊), angular momentum L (△), enstrophy Z_2 (■) and palinstrophy P (▼). Inset: The time evolution of the viscosity coefficients estimated experimentally (○) and calculated from Eq. (62) in Ref. [16] (●).

derive the spectrum in the stationary state through time-averaging the evolution of spectra and compare with the Kraichnan-Batchelor theory.

The experiment is carried out by containing a pure electron plasma in a Malmberg-trap with a uniform magnetic field ($B_0 = 0.048$ T) and a square-well potential. After the plasma is formed into a ring-shaped profile, the density distribution at a specific time in the relaxation process is observed by damping the electrons onto the conducting phosphor screen and recording the luminosity distribution with a 512×512 pixel CCD camera providing the spatial resolution of 0.1 mm/pix. This destructive diagnostic requires a high reproducibility of the initial profiles, because the relaxation process of the turbulence triggered by the instability is stochastic in nature. Therefore in this experiment, in addition to technically minimizing shot-by-shot variations in the initial profiles, an ensemble-average is applied over typically 5 shots of data for each time of the observation in examining the time evolution of physical quantities characterizing the turbulence. The details of the experimental configuration and method are reported in Refs. [4, 6, 12, 13].

The time evolution of the observed density distribution is shown in Fig. 1. The ring profile is produced at 5 μs, and distorted by the diocotron instability within a few μs. The deformed distribution grows on the fastest growing diocotron mode and eventually 5 high-density vortex patches are generated at 13 μs. After the formation of the first vortex patches, the number of patches decreases successively through intermittent mergers among the patches. This stochastic process is accompanied by the generation of filamentary structures in the low density part of the population that extend the length-scales to finer regions. The outward transport of the filamentary structures is accompanied by the inward transport of the high-density patches as observed at 31 μs. The concentrated patches rotating with the period of 10 μs expel filaments from the central region, and finally form a bell-shaped core distribution that is surrounded by a low density halo with striations ($t = 200$ μs).

Turbulent states are characterized by areal integrals of the vorticity ($\propto n(x, y)$). Figure 2 plots some of the integrals calculated from the measured density distribution $n(r, \theta)$ as a function of time. Each integral is normalized to unity. The integrals include the electrostatic energy (fluid kinetic energy) $E = 1/2 \int d^2\mathbf{r} n\,(-e\phi)$, the total electron number (total circulation) $N = \int d^2\mathbf{r} n$, the angular momentum (angular impulse) $L = \int d^2\mathbf{r} n r^2$, the enstrophy $Z_2 = 1/2 \int d^2\mathbf{r} n^2$ and the palinstrophy $P = 1/2 \int d^2\mathbf{r}\, |\nabla n|^2$. The palinstrophy is a measure of the fine-scale structures in the turbulence [8, 9, 14].

Throughout the whole process, E, N and L do not show any systematic change except 5 % variations probably attributable to the shot-by-shot fluctuations in the generation process of the unstable initial distributions. Therefore the three integrals may be considered to be invariant. In contrast, Z_2 and P show unambiguous systematic changes. The enstrophy Z_2 undergoes a substantial decaying through the merging processes, and finally goes down to 40 % of the initial value. The palinstrophy P shows a rapid increase while mergers among the vortex patches are active. It is maximized at 31 μs when the filamentary structures are conspicuous in the region outside the high-density core as shown in Fig. 1. After the maximization, P drops steeply concomitantly with the reduction of the decreasing rate of the enstrophy, suggesting the manifestation of dissipative effects in finer length-scales.

In order to estimate the degree of enstrophy dissipation in this experiment, we introduce a Newtonian viscosity into the 2D Euler equation as a correction, i.e., $Dn/Dt = \nu \nabla^2 n$, where ν is the kinematic viscosity. (Note that n is propotional to the vorticity.) This equation leads to the relation of the decreasing rate of the enstrophy to the viscosity and palinstrophy as follows [8, 9, 14]:

$$\frac{DZ_2}{Dt} = -2\nu P \tag{1}$$

By introducing the experimental values of Z_2 and P into Eq. (1), the effective viscosity ν is evaluated and plotted as a function of time in Fig. 2. ν is maximized at time $t \approx 23$ μs when the density configuration changes drastically from separated vortex patches to a single-peaked distribution.

The collisional transport of a magnetized pure electron plasma in the 2D regime [15] has been studied analytically, in which the viscosity coefficient is predicted as Eq. (62) in Ref. [16]. By introducing the parameters of the present experiment to the proposed formula, we estimate the viscosity coefficient ν_{th} and plot the results in Fig. 2. Though the present study is not under quasi-stationary states as assumed in the theory, the experimental evaluation agrees within a factor of 2 with ν_{th}. This agreement may suggest that the stochastic motions of individual particles under fluctuating fields play a important role in the dissipation process of vortex dynamics in fine scales.

To compare the experimental results to the theoretical picture of 2D turbulence, we calculate the energy spectrum in k space from the measured density distribution. The energy spectrum $E(k)$ is determined from the Fourier transform of the density distribution $n(\mathbf{k}) = \int d^2\mathbf{r}e^{-i\mathbf{k}\cdot\mathbf{r}}n(\mathbf{r})$ as

$$E(k) = \frac{1}{2}\left(\frac{e}{\varepsilon_0 B_0}\right)^2 \int_0^{2\pi} kd\varphi \frac{|n(\mathbf{k})|^2}{k^2}, \qquad (2)$$

where φ is the azimuthal angle of $\mathbf{k}$. The time evolution of $E(k)$ thus obtained is shown in Fig. 3. In the initial distribution at 5 μs, the energy spectrum shows oscillatory structures due to the concentration of the energy at the ring radius. When the ring distribution is torn into the vortex patches at 13 μs, the spectrum has a local maximum around the wave number $k = k_{inj} \approx 500$ consistent with the size of the first vortex patches. Along with the subsequent mergers between patches ($t = 13 \sim 31$ μs), the location of the spectral maximum shifts progressively down to lower wave numbers, and the dip around $k \equiv k_{core} \approx 300$ which corresponds to the core size in the final state is filled.

In length-scales smaller than the width of the vortex patches $k > k_{inj}$, the energy spectrum broadens upward and the $E(k)$ exhibits a power-law dependence of $\propto k^{-\alpha}$. The slope of the spectrum in the interval $700 \leq k \leq 5000$ is drawn in Fig. 3. Throughout the merging processes, the power index α remains around 5, apparently larger than the theoretically predicted value of 3 [8]. The upper limit in the wave-number space $k = k_d$ to which $E(k)$ shows a power-law scaling reaches its maximum value of ≈ 8300 at 31 μs when the palinstrophy is maximized. This scale-length (≈ 0.38 mm) is consistent with the thickness of the filamentary structure at the end of spiral arms displayed in Fig. 1.

In the slow relaxation process toward the asymptotic state after the merger ($t = 40 \sim 200$ μs), the energy concentrates at k_{core} and decreases steeply beyond $k \approx 1000$. The power index in the high wave-number region $1000 \leq k \leq 5000$ decreases slowly from ≈ 5 toward 3.5. The power-law spectrum at high k represents fine structures remaining in the halo region surrounding the high density core.

The rate of upward energy transfer $\varepsilon(k)$ through k is evaluated from the time-resolved energy spectrum in Fig. 3 as

$$\varepsilon(k) = -\int_0^k dk\ \frac{\partial E(k)}{\partial t}. \qquad (3)$$

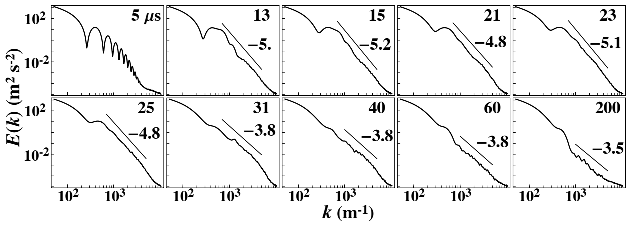

Fig. 3 The time evolution of the energy spectrum calculated from the measured $n(\mathbf{r})$. Numbers at the upper-left corner stand for the time of the observation.

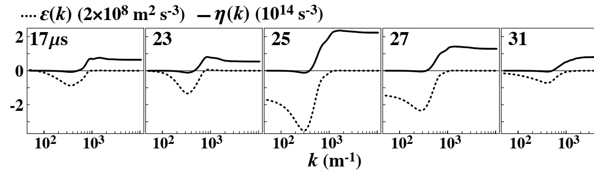

Fig. 4 The time evolution of the upward transfer rates of the energy $\varepsilon(k)$ (dashed line) and enstrophy $\eta(k)$ (solid line) through k.

The enstrophy transfer rate $\eta(k)$ is evaluated similarly from the enstrophy spectrum $Z(k) = k^2E(k)$. The time evolution of $\varepsilon(k)$ and $\eta(k)$ during the period in which $E(k)$ follows the power-law is shown in Fig. 4. The observation of $\varepsilon(k)$ indicates that the energy is transfered downward and the rate of transfers is maximum around k_{core} at each time. In contrast, the enstrophy is transferred upward in the wave-number space with $k \geq k_{inj}$. In particular, over the wide range of $k \geq 1500$, $\eta(k)$ is almost constant as assumed in the theoretical picture of 2D turbulence. Both in the energy and in the enstrophy, the transfer rates are maximized at $t \approx 25$ μs when the density configuration changes drastically.

The observation that $\eta(k)$ decreases to zero at $k < 2k_{inj}$ from a constant value at $k > 3k_{inj}$ corresponds to the observed vortex dynamics in Fig. 1, i.e., the vortex patch retain its shape for a long time with high vorticities (enstrophy) and the filamentation of the structure dominates in the outside region of the patches.

The time-resolved data presented above include details of free-decaying 2D turbulence whose enstrophy is fed at $k = k_{inj}$ corresponding to the first generation of vortex patches and that is left in an isolated state. Here we try to construct the energy spectrum in a stationary state that is maintained by continuous energy input at $k = k_{inj}$ due to the instability and by the continuous dissipation at $k \gg k_{inj}$ by using the above data as an elementary process constituting a stationary turbulence. If the interaction among the structures appearing in different stages of the free-decaying turbulence is negligible, the time-averaged spectra, $\bar{E}(k)$, $\bar{\varepsilon}(k)$ and $\bar{\eta}(k)$, may approximately represent the characteristic features of the stationary turbulence. The results of the time-weighted average of the observed data are summarized in Fig. 5.

The constructed spectra exhibit characteristics close to the fundamental features of stationary 2D turbulence:

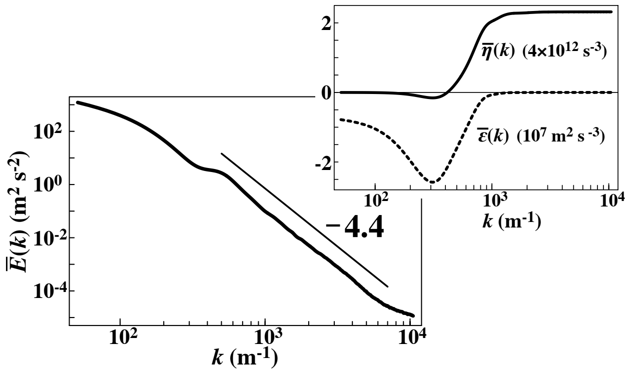

Fig. 5 The energy spectrum $\bar{E}(k)$ time-averaged in the interval $t = 13 \sim 200$ μs. Inset shows the time-averaged transfer rates of the energy $\bar{\varepsilon}(k)$ (dash line) and enstrophy $\bar{\eta}(k)$ (solid line).

The enstrophy is transfered upward at a constant rate above $k \approx 3k_{inj}$. With this transfer rate, the dissipative wave number is estimated at $k_d \approx 7200$ from the expression $l_d \approx \eta^{-1/6}\nu^{1/2}$ proposed in Ref. [8]. Figure 5 also shows that $\bar{E}(k)$ depends algebraically on k in a wide range of the wave-number space $k_{inj} \leq k \leq k_d$. In contrast to $\bar{\eta}(k)$, it is confirmed that in the region $k < 3k_{inj}$, the energy flux $\bar{\varepsilon}(k)$ proceeds toward small wave-numbers and is maximized around k_{core} corresponding to the size of the core distribution in the asymptotic state.

Through the region $k \geq 3k_{inj}$ where the enstrophy transfer rate is constant, the energy transfer rate is observed to be zero. This observation supports the theoretical expectations that the spectral dynamics at high wave-numbers of the 2D turbulence are governed by the enstrophy cascade process [7]. On the other hand, in the region $k < k_{inj}$, the observation that $\bar{\eta}(k) \sim 0$ and $\bar{\varepsilon}(k) < 0$ indicates that the dynamics in the energy spectra obey the inverse cascade process. The observed non-uniformity of $\bar{\varepsilon}(k)$ is understood in terms of the absence of a dissipation mechanism at large length-scales in the strongly magnetized pure electron plasma.

In the intermediate region $k_{inj} \leq k < 3k_{inj}$, neither $\bar{\varepsilon}(k)$ nor $\bar{\eta}(k)$ is zero, indicating that the transfer exists in the k space of both the energy and enstrophy. The local non-uniformity of $\bar{\varepsilon}(k)$ and $\bar{\eta}(k)$ in this region suggests the break-down of the ubiqitous cascade model. This observation is closely related to the persisting presence of coherent vortices that capture a large amount of enstrophy and inhibit the cascade as observed by numerical simulations [17, 18]. This is probably the reason why the power index of the observed energy spectrum $\bar{E}(k)$ in the inertial range of $k_{inj} \leq k \leq k_d$ is $\alpha = 4.4$ and larger than the theoretical prediction of $\alpha = 3$ [7].

In this paper, we have examined the vortex dynamics of 2D turbulence in a magnetized pure electron plasma over a wide range of length-scales extending from the injection scale down to the dissipative scale, and compared the experimental results to existing theories of 2D turbulence. In the stage characterized by the successive mergers between vortex patches starting from the unstable initial density profile, the observed density distribution exhibits turbulent characteristics. While the energy is transfered downward, the enstrophy undergoes an upward transport starting from the injection wave number k_{inj}. In finer length-scales with $k \geq 3k_{inj}$, the transfer rate of the enstrophy is observed to be constant, and the energy spectrum shows a power-law scaling $E(k) \propto k^{-\alpha}$ in a broad inertial range with α ranging from 5.2 to 3.5. The discrepancy from the theoretically-expected value of $\alpha = 3$ is attributed to the inhibition of the cascade process reflecting the effect of the long persistence of high-vorticity patches.

The author thanks Professor K. Itoh of NIFS for enlightening discussions. This research was supported by the Grant-in-Aid for Scientific Research (B) 17340173 of JSPS and partly by the collaborative program of NIFS.

[1] R. H. Levy, Phys. Fluids **8**, 1288 (1965).
[2] C. F. Driscoll and K. S. Fine, Phys. Fluids B **2**, 1359 (1990).
[3] T. B. Mitchell and C. F. Driscoll, Phys. Fluids **8**, 1828 (1996).
[4] Y. Kiwamoto, K. Ito, A. Sanpei and A. Mohri, Phys. Rev. Lett. **85**, 3173 (2000).
[5] A. J. Peurrung and J. Fajans, Phys. Fluids A **5**, 493 (1993).
[6] Y. Kawai, Y. Kiwamoto, K. Ito, A. Sanpei, Y. Soga, J. Aoki and K. Itoh, J. Phys. Soc. Jpn. **75**, 104502 (2006).
[7] R. H. Kraichnan, Phys. Fluids **10**, 1417 (1967).
[8] G. K. Batchelor, Phys. Fluids **12** (Suppl.II), 233 (1969).
[9] P. Tabeling, Physics Reports **362**, 1 (2002).
[10] J. Paret, M. C. Jullien, P. Tabeling, Phys. Rev. Lett. **83**, 3418 (1999).
[11] M. A. Rutgers, Phys. Rev. Lett. **81**, 2244 (1998).
[12] K. Ito, Y. Kiwamoto and A. Sanpei, Jpn. J. Appl. Phys. **40**, 2558 (2001).
[13] J. Aoki, Y. Kiwamoto, Y. Soga and A. Sanpei, Jpn. J. Appl. Phys. **43**, 7267 (2004).
[14] U. Frisch, *TURBULENCE* (Cambridge University Press, Cambridge, 1995).
[15] C. F. Driscoll, F. Anderegg, D. H. E. Dubin, D.-Z. Jin, J. M. Kriesel, E. M. Hollmann and T. M. O'Neil, Phys. Plasmas. **9**, 1905 (2002).
[16] D. H. E. Dubin and T. M. O'Neil, Phys. Plasmas. **5**, 1305 (1998).
[17] J. C. McWilliams, J. Fluid Mech. **146**, 21 (1984).
[18] P. Santangelo, R. Benzi and B. Legras, Phys. Fluids A **1**, 1027 (1989).